



Contents lists available at ScienceDirect

# Chaos, Solitons and Fractals

Nonlinear Science, and Nonequilibrium and Complex Phenomena

journal homepage: [www.elsevier.com/locate/chaos](http://www.elsevier.com/locate/chaos)

## On the analysis of pseudo-orbits of continuous chaotic nonlinear systems simulated using discretization schemes in a digital computer

Erivelton Geraldo Nepomuceno<sup>a,\*</sup>, Eduardo M.A.M. Mendes<sup>b</sup><sup>a</sup> Model and Control Group (GCOM), Department of Electrical Engineering, Federal University of São João del-Rei, São João del-Rei, MG, 36307-352, Brazil<sup>b</sup> Department of Electronic Engineering, School of Engineering, Federal University of Minas Gerais, Belo Horizonte, MG, 31270-901, Brazil

### ARTICLE INFO

#### Article history:

Received 25 May 2016

Revised 14 October 2016

Accepted 7 December 2016

Available online 16 December 2016

#### Keywords:

Nonlinear dynamics systems

Chaos

Discretization schemes

Pseudo-Orbit

Lower bound error

Lyapunov exponent

### ABSTRACT

This paper reports the existence of more than one pseudo-orbit when simulating continuous nonlinear systems using a digital computer in a set-up different from the ones normally seen in the literature, that is, in a set-up where the step-size is not varied, the discretization scheme is kept the same as well as the initial conditions. Taking advantage of the roundoff error, a simple but effective method to determine a lower bound error and the critical time for the pseudo-orbits is used and the connection to the maximum (positive) Lyapunov exponent is established considering the bit resolution and the computational platform used for the simulations. To illustrate the effectiveness of the method and problems of using discretization schemes for simulating continuous nonlinear systems in a digital computer, the well-known Lorenz equations, the Rossler hyperchaos system, Mackey–Glass equation and the Sprott A system are used. The method can help the user of such schemes to keep track of the reliability of numerical simulations.

© 2016 Elsevier Ltd. All rights reserved.

### 1. Introduction

Numerical computation plays a key role in analysing the solutions of nonlinear dynamical systems [8,11,28,48]. Numerical experiments [42] have been used since the seminal work of Lorenz [25] in order to understand complex nonlinear dynamical systems that exhibit chaotic behaviour. As a result, researchers have been identifying chaotic behaviour [41] in various systems by analysing the generated numerical solutions. These solutions are obtained using discretization schemes available in popular software and computers easily accessible to most researchers. However, as stated in [28], there are many published works in which the reliability of numerical results is not carefully verified. The same author states that “In the simple case of a dynamic discrete system (of Hénon map), there are doubts as to the nature of the computational results: long unstable pseudo-orbits or strange attractors?”.

At first sight the natural way to deal with the problem would be to borrow and adapt the results of earlier works on the linear case. However, this approach should be used with care since there are important differences between the linear case and the nonlinear case. One of the first papers to deal with the problem

of roundoff errors for the linear case in a digital computer is [46], where the author studies the effects of roundoff in the floating-point realization of a general *linear* discrete filter governed by a *stable* difference equation. Further works on this direction with the objective of understanding and minimizing the roundoff error are [14,32,36,37,50] just to mention a few. Although limit cycles have been reported due to the roundoff [4,13,32], the basic idea was to design filter structures to reduce roundoff noise and coefficient sensitivity, avoid overflow oscillations and quantization limit cycles when magnitude truncation is employed. The problem of structural instabilities for the linear continuous case was studied in [34]. These results are useful to understand some consequences of the roundoff error but their extension to the nonlinear case is not completely obvious.

In the investigation of some of aforementioned problems in the context of nonlinear systems, Lorenz [26] coined the term “Computational Chaos” while studying the chaotic behaviour of difference equations used to approximate a continuous system represented by a set of differential equations as the step-size is increased. Further results on the same subject can be found in [8,18,27,53]. Lao [18], for instance, has introduced the concept of critical predictable time to provide a more precise description of computed chaotic solutions of nonlinear differential equations. The author has suggested that the computed solutions, using discretization schemes, can not lead to accurate long-term prediction of chaotic time-series beyond the critical predictable time. He has also pointed out that

\* Corresponding author.

E-mail addresses: [nepomuceno@ufsj.edu.br](mailto:nepomuceno@ufsj.edu.br) (E.G. Nepomuceno), [emmendes@cpdee.ufmg.br](mailto:emmendes@cpdee.ufmg.br) (E.M.A.M. Mendes).

two digitally computed chaotic outputs generated by different discretization schemes differs after the critical predictable time even if the used initial conditions are exactly the same. In a similar way, Corless [5] points out four levels of abstraction when one is dealing with modelling: “the physical reality of the problem under study, the continuous mathematical model of that physical reality, the numerical discretization of that mathematical model, and the floating-point simulation of that discretization”. Regarding specifically to nonlinear dynamics, Corless [5] is still more incisive when stating that “Results from one level may or may not transfer easily to another level, and in particular, even qualitative features may not be preserved in that transfer. Moreover, there is no inherent bias either way: in any change of level we can introduce or destroy chaos.”

Having in mind not the occurrence of different solutions due to the increase of the step-size or to the use of different discretization schemes but due to the numerical solution itself, Nepomuceno [39] has shown that a simple sequence of iterations of a well-known nonlinear system can reach a steady state value that is not the theoretical one. In other words, the sequence did not converge to the theoretical value due to numerical issues. In the same work, a method to calculate the propagation of error in the computation of recursive function is presented. The investigation of propagation error is not a recent issue (See for instance [6,10,11]) but, in fact, there are many works based on deterministic or statistical tools that provide some confidence when simulating recursive functions. Analysing such functions, Nepomuceno [39] has calculated the propagation of the error based on the evaluation of the sequence of arithmetic functions and Taylor expansion. Although, the results seem reasonable, the application of such technique is not practical for recursive functions with many terms, such as nonlinear discrete models [3], or discretization schemes for obtaining the numerical solutions for nonlinear differential equations when the goal is to measure or, at least, to estimate the error.

In order to investigate the error in complex recursive functions, Nepomuceno and Martins [40] introduced an approach to evaluate a lower bound error based on the fact that although interval extensions [35] are mathematically equivalent, they may generate different computer simulation outcomes. The result of using multiple interval extensions is the introduction of a new concept, “multiple pseudo-orbits”, that differs from the general view that a simulation generated by iterating nonlinear systems exhibits only one pseudo-orbit. To compare the generated pseudo-orbits to the true one, Hammel et al. [11] have shown that the latter exists near a pseudo-orbit using mathematical analysis. In a somehow similar context, this paper explores the lower bound error to the context of continuous nonlinear systems simulated using discretization schemes. The lower bound error, that is, an inferior limit for the error, has a direct consequence on the understanding of the solutions generated by nonlinear dynamical systems. By means of a very simple change in the equation to be simulated, that is, by applying a distributive property, two different pseudo-orbits are produced even when the initial conditions and step size are not varied.

To further emphasize the main point of the present work, consider a recent work in which it is addressed the issue of obtaining chaotic solutions in a finite interval of time using symbolic computation, extremely high-order Taylor expansion and a super computer [22]. The author states that “... because Lorenz [26,27] further found that chaotic solutions are sensitive not only to initial conditions but also to numerical algorithms: different numerical algorithms with different time-steps may lead to completely different numerical results of chaos”. The present paper goes beyond that, when it states that even when the initial conditions are exactly the same, the algorithm is not changed and the step time is kept unchanged, one can find multiple pseudo-orbits simply by

changing the way the model is written. Instead of trying to give a full answer to question “which pseudo-orbit is more correct?”, guidelines are provided to help the user of discretization schemes to analyse the variety of numerical solutions and to establish a relationship between the different pseudo-orbits and the maximum (positive) Lyapunov exponent when possible.

The rest of the paper is laid out as follows: In Section 2, two discretization schemes are briefly reviewed. The proposed method based on the lower bound error is presented in Section 3. To illustrate this approach, examples using the well-known Lorenz equations, the Rossler hyperchaos system, Mackey–Glass Equation and the Sprott A system are given in Section 4. Section 5 presents the conclusions.

## 2. Discretization schemes

Two discretization schemes are now briefly reviewed. The first scheme is the well-known Runge–Kutta of 4th order, usually referred to as RK4 [43]. Consider an initial value problem specified as follows:

$$\dot{x} = f(t, x), \quad x(t_0) = x_0, \quad (1)$$

where  $x$  is some state variable (or output signal).

With a step-size (or discretization step)  $h > 0$  the RK4 can be expressed as

$$x_{n+1} = x_n + \frac{h}{6}(k_1 + 2k_2 + 2k_3 + k_4), \quad (2)$$

where

$$\begin{aligned} K_1 &= f_n, \\ K_2 &= f\left(t_n + \frac{h}{2}, x_n + \frac{h}{2}K_1\right), \\ K_3 &= f\left(t_n + \frac{h}{2}, x_n + \frac{h}{2}K_2\right), \\ K_4 &= f(t_{n+1}, x_n + hK_3). \end{aligned} \quad (3)$$

The second method investigated is the Monaco and Normand-Cyrot Discretization Scheme [33]. Let the dynamic system be

$$\dot{\mathbf{x}} = \mathbf{f}(\mathbf{x}), \quad (4)$$

where  $\mathbf{x} = (x_1, \dots, x_m) \in \mathbb{R}^m$  are state variables,  $\mathbf{f}(\cdot)$  are (differentiable) functions.

Here an alternative procedure for discretization of Eq. (4) as described in [2] is given. A discrete model of Eq. (4) can be written as

$$\mathbf{x}_{k+1} = \mathbf{g}(\mathbf{x}_k, h), \quad (5)$$

where  $\mathbf{x}_k \in \mathbb{R}^m$  are the discrete state variable at time  $t = t_0 + kh$  and  $t_0$  is the initial time.

In [19,30], the Monaco and Normand-Cyrot discretization scheme was obtained by the Lie exponential expansion of Eq. (4) as follows:

$$\mathbf{x}_{k+1} = \mathbf{x}_k + \sum_{n=1}^{\eta} \frac{h^n}{n!} L_f^n(\mathbf{x}_k), \quad (6)$$

where  $\eta$  is the expansion order. The Lie derivative is given by:

$$L_f(\mathbf{x}_k) = \sum_{j=1}^m f_j \frac{\partial \mathbf{x}}{\partial x_j}, \quad (7)$$

where  $f_j$  represents the  $j$ th component of the vector field. Higher order derivative orders can be calculated by:

$$L_f(\mathbf{x}_k) = L_f(L_f^{n-1}(\mathbf{x}_k)). \quad (8)$$

All simulations are performed on an IBM PC-compatible machine using Matlab R2016a or Fortran. All routines used in this work are available upon request.

### 3. The lower bound error and the critical time

This section is an adaptation and an extension of the work of Nepomuceno and Martins [40] on the lower bound error applied to continuous nonlinear systems. First some definitions on recursive functions, interval extension and pseudo-orbits are introduced. After that, the theorem of lower bound error, which has been proved in [40], is presented.

Let  $n \in \mathbb{N}$ , a metric space  $M \subset \mathbb{R}$ , the relation

$$x_{n+1} = f(x_n), \tag{9}$$

where  $f: M \rightarrow M$ , is a recursive function or a map of a state space into itself and  $x_n$  denotes the state at the discrete time  $n$ . The sequence  $\{x_n\}$  obtained by iterating Eq. (9) starting from an initial condition  $x_0$  is called the orbit of  $x_0$  [9].

Let  $f$  be a function of real variable  $x$ . Moore and Moore [35] presents the following definition.

**Definition 3.1.** An interval extension of  $f$  is an interval valued function  $F$  of an interval variable  $X$ , with the property

$$F(x) = f(x) \quad \text{for real arguments,} \tag{10}$$

where by an interval we mean a closed set of real numbers  $x \in \mathbb{R}$  such that  $X = [\underline{X}, \bar{X}] = \{x : \underline{X} \leq x \leq \bar{X}\}$ .

**Definition 3.2.**  $G$  and  $H$  are equivalent interval extensions if

$$G(X) = H(X) \quad \text{for interval arguments.}$$

Consider the following example of Definition 3.2.

**Example 3.3.** Let the following extension intervals:

$$\begin{aligned} G(X) &= rX(1 - X) \\ H(X) &= r(X(1 - X)) \\ L(X) &= rX - rX^2. \end{aligned}$$

Considering  $r = 4$  and  $X = [0.1, 0.2]$  yields

$$\begin{aligned} G([0.1, 0.2]) &= 4[0.1, 0.2](1 - [0.1, 0.2]) = [0.32, 0.72], \\ H([0.1, 0.2]) &= 4([0.1, 0.2](1 - [0.1, 0.2])) = [0.32, 0.72] \quad \text{and} \\ L([0.1, 0.2]) &= 4[0.1, 0.2] - 4([0.1, 0.2]^2) = [0.24, 0.76]. \end{aligned}$$

In this example only  $G(X)$  and  $H(X)$  are equivalent interval extensions.

Associated to a map an orbit may be defined as follows:

**Definition 3.4.** An orbit is a sequence of values of a map, represented by  $\{x_n\} = [x_0, x_1, \dots, x_n]$ .

There is no unique pseudo-orbit, as there are different hardware, software, numerical precision standard and discretization schemes, which may yield different output for each extension interval.

**Definition 3.5.** Let  $i \in \mathbb{N}$  represents a pseudo-orbit, which is defined by an initial condition, an interval extension of  $f$ , some specific hardware, software, numerical precision standard and discretization scheme. A pseudo-orbit is an approximation of an orbit and can be represented as

$$\{\hat{x}_{i,n}\} = [\hat{x}_{i,0}, \hat{x}_{i,1}, \dots, \hat{x}_{i,n}],$$

such that

$$|x_n - \hat{x}_{i,n}| \leq \delta_{i,n}, \tag{11}$$

where  $\delta_{i,n} \in \mathbb{R}$  is the error and  $\delta_{i,n} \geq 0$ .

A pseudo-orbit defines an interval where the true orbit sits. Hence an interval associated with each value of a pseudo-orbit may be defined as

$$I_{i,n} = [\hat{x}_{i,n} - \delta_{i,n}, \hat{x}_{i,n} + \delta_{i,n}]. \tag{12}$$

From (11) and (12) it is clear that

$$x_n \in I_{i,n}, \quad \text{for all } i \in \mathbb{N}. \tag{13}$$

**Theorem 3.6 [40].** Let two pseudo-orbits  $\{\hat{x}_{a,n}\}$  and  $\{\hat{x}_{b,n}\}$  derived from two interval extensions. Let  $\delta_{\alpha,n} = \frac{|\hat{x}_{a,n} - \hat{x}_{b,n}|}{2}$  be the lower-bound error of a map  $f(x)$ , then  $\delta_{a,n} \geq \delta_{\alpha,n}$  or  $\delta_{b,n} \geq \delta_{\alpha,n}$ .

Theorem 3.6 establishes that at least one of the two pseudo-orbits must have an error greater or equal to the lower-bound error. This has a practical meaning. If this lower-bound error is greater than the required precision, the simulation should not be carried on without further analysis. It should kept in mind that simulation of a continuous nonlinear system using a discretization scheme presents multiple pseudo-orbits, to which Theorem 3.6 can be directly applied.

The analysis on the pseudo-orbits described here is carried out based on two aspects. First, it is taken into account the very definition of chaotic systems proposed by Devaney and therefore errors will eventually lead to large scale divergence [1]. Second, a very simple strategy to produce a measure related to these errors is presented using only heuristic arguments. Following this rationale, note that the lower bound error is a measure of the distance between the simulated dynamical systems (or pseudo-orbit) and the real orbit. If a system behaves chaotically the distance between these two entities must be exponentially divergent, and therefore a slope in a logarithm plot of the lower bound error is what is needed to capture such a divergence and quantified it as a number which is precisely the definition of the positive Lyapunov exponent (For more details the reader is referred to [31]).

Since all simulations performed in a digital computer should, in principle, follow IEEE 754-2008 norm, some of its contents should be observed. They are: “This standard provides a discipline for performing floating-point computation that yields results independent of whether the processing is done in hardware, software, or a combination of the two.” and “Floating-point arithmetic is a systematic approximation of real arithmetic (...) and certain properties of real arithmetic, such as associativity of addition, do not always hold for floating-point arithmetic.” Based on these statements the following lemma can be derived.

**Lemma 3.7.** Two interval extensions starting from the same initial condition eventually produces a different result at the same time  $n$ .

**Proof.** Suppose that the contrary is true, then the two interval extensions produces the same result for all  $n$ . Since they are not exactly the same, this contradicts the statement of the IEEE 754-2008 norm that states that there is no guarantee that basic arithmetic properties, such as the distributive property, hold. This leads to absurd and completes the proof.  $\square$

With this in mind, it is clear that, for chaotic systems, two interval extensions will diverge and the critical time when the orbits reach the maximum distance can be established as shown in the following lemma.

**Lemma 3.8.** Let a chaotic system be described by function  $f(n)$ . Let  $g(n)$  be an interval extension of  $f(n)$ . Then  $\delta_{\alpha,n} \leq D/2$  as  $n \rightarrow N_c$ , where  $D$  is the diameter of the phase space and  $N_c$  is a critical time or number of iterates, where the simulation loses the significance of all digits.

**Proof.** Lemma 3.7 establishes that  $f(n)$  and  $g(n)$  will eventually produce different results, even from the same initial condition. For chaotic system, this means that the results will diverge from each other. The maximum distance between these two pseudo-orbits is the diameter of the phase space and therefore the lower bound error is limited to the half of this value. The critical time  $N_c$  may be calculated using the value of the largest Lyapunov Exponent and

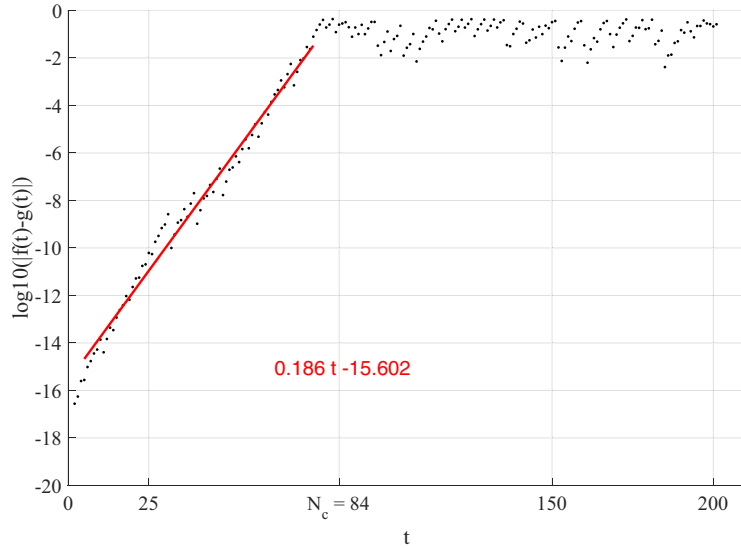


**Fig. 1.** Illustration of Lemma 3.8 for the logistic map. The largest Lyapunov exponent is given by the inclination of the fitted line, that is,  $\lambda = 0.186$  (here measured in base 10). The critical time  $N_c = 84$  is also indicated in the figure.

the precision,  $P$ , of the simulation as follows

$$N_c = \frac{\log_{10}(D/2) + P}{\lambda}.$$

This completes the proof.  $\square$

To illustrate Lemma 3.8 consider the following example.

**Example 3.9.** Let the logistic map with the following two interval extensions  $x_{n+1} = f(x_n) = rx_n(1 - x_n)$  and  $x_{n+1} = g(x_n) = rx_n - rx_n x_n$ , where  $r = 3.9$  and  $x_0 = 0.1$ . The lower bound error and Lyapunov exponent ( $\lambda = 0.186$ ) are shown in Fig. 1 (for the sake of simplicity logarithm base 10 is used). Let  $D = 1$  and  $P \approx 16$ , since the logistic equation was simulated on a 64-bit Matlab R2016a environment, then

$$N_c = \frac{\log_{10}(1/2) + 16}{0.186} = 84.4. \tag{14}$$

Note that i)  $N_c \approx 84$  is in very good agreement with the value shown in Fig. 1, ii) the line fitted to the curve gives the Lyapunov exponent and iii) the independent term, 15.6, gives a good estimation of the precision  $P$ .

In the next section illustrative examples will be given to demonstrate the usefulness of the main ideas of the paper.

#### 4. Illustrative examples

Consider the Lorenz equations [25] defined by the following set of differential equations

$$\begin{aligned} \frac{dx}{dt} &= \sigma(y - x) \\ \frac{dy}{dt} &= x(\rho - z) - y \\ \frac{dz}{dt} &= xy - \beta z. \end{aligned} \tag{15}$$

The Lorenz equations in (15) can be numerically solved using the discretization schemes reviewed in Section 2.

It is worth emphasizing that any other chaotic system can be used to illustrate the main ideas of this paper. Therefore the main point is not show that the lower bound error can be applied to the Lorenz equations, but to any chaotic system and more than that to any discretization scheme. This will be clear in the next subsections.

#### 4.1. Equivalent interval extensions of the Lorenz equations

Consider now two equivalent interval extensions of Eq. (15) given by

$$\begin{aligned} \frac{dx_1}{dt} &= \sigma(y_1 - x_1) \\ \frac{dy_1}{dt} &= \underline{x_1}(\rho - z_1) - y_1 \\ \frac{dz_1}{dt} &= x_1 y_1 - \beta z_1 \end{aligned} \tag{16}$$

and

$$\begin{aligned} \frac{dx_2}{dt} &= \sigma(y_2 - x_2) \\ \frac{dy_2}{dt} &= \underline{x_2} \rho - x_2 z_2 - y_2 \\ \frac{dz_2}{dt} &= x_2 y_2 - \beta z_2. \end{aligned} \tag{17}$$

Note that the two set of equations, Eqs. (16) and (17), are mathematical equivalent. However, they are written slightly different, as indicated by the underline terms and they will be shown to exhibit different outcomes. To this end, consider the solution of the Lorenz equations with  $\sigma = 10$ ,  $\rho = 28$  and  $\beta = 8/3$ , initial conditions  $(x_0, y_0, z_0) = (0, 1, 1.05)$  and step-size  $h = 0.005$  for both Eqs. (16) and (17). Fig. 2 shows the result for variable  $x_1$  and  $x_2$  for  $t \in [40, 60]$  considering that no modification was implemented on the code of routine *ode4*. As can be seen, just before  $t = 48$  LTU (Lorenz Time Units [53]), the two pseudo-orbits diverge from each other significantly. Actually they grow apart exponentially as shown in Fig. 3.

In particular, for the first point  $t_1$  greater that  $t = 47$  LTU, the lower error bound using these two pseudo-orbits is

$$\delta_{\alpha, t_1} = \frac{|\hat{x}_{1, t_1} - \hat{x}_{2, t_1}|}{2} = \frac{|-1.237 - (-2.074)|}{2} = 0.4185, \tag{18}$$

which is a considerable error of around 20% of absolute value of  $\hat{x}_{2, t_1}$ .

#### 4.2. RK4 - equivalent interval extensions of the discretization scheme

In the second example, Eq. (16) is considered and the code of the discretization scheme, that is RK4, is modified by applying

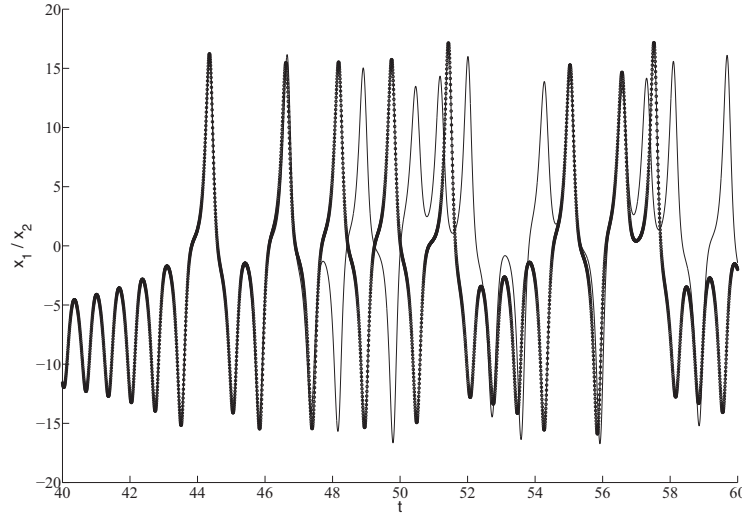


**Fig. 2.** Result of simulation for  $x_1$  (—) and  $x_2$  (---). The simulation is performed using the set of Eqs. (16) for  $x_1$  and (17) for  $x_2$ . The parameters  $\sigma = 10$ ,  $\rho = 28$ ,  $\beta = 8/3$ , step-size  $h = 0.005$  and initial conditions  $(x_0, y_0, z_0) = (0, 1, 1.05)$  are exactly the same.

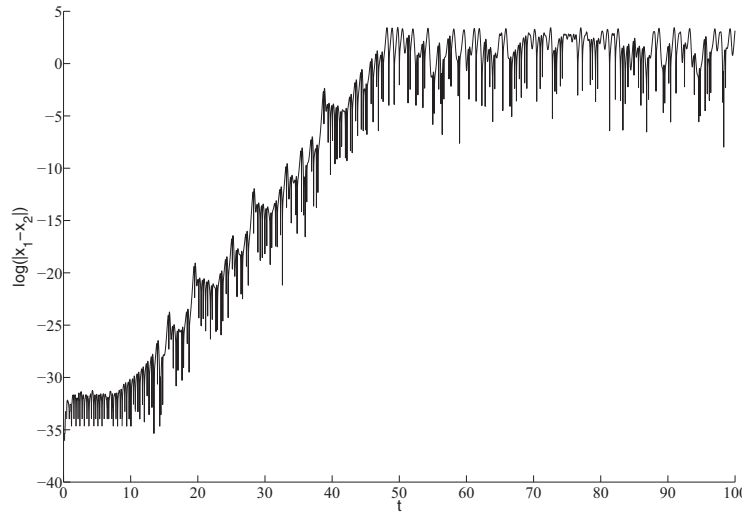


**Fig. 3.** Exponentially growing of the difference between the two pseudo-orbits  $x_1$  and  $x_2$ , as seen in Fig. 2.

the distributive property. The modification was implemented by changing the following line from

$$Y(:, i) = yi + (hi/6) * (F(:, 1) + 2 * F(:, 2) + 2 * F(:, 3) + F(:, 4));$$

to

$$Y(:, i) = yi + (hi/6) * (F(:, 1) + 2 * (F(:, 2) + F(:, 3)) + F(:, 4));$$

Observe that the unique change is mathematically equivalent, as

$$2 * F(:, 2) + 2 * F(:, 3) = 2 * (F(:, 2) + F(:, 3)).$$

Although the mathematical equivalence, this simple change can result in two different pseudo-orbits as can be seen in Fig. 4. The same pattern shown in the first case is also observed here. The error grows exponentially and eventually becomes large enough to provoke a very different outcome (See Fig. 5).

#### 4.3. Monaco and Normand Cyrot scheme - equivalent interval extensions of the Lorenz Equations

The third illustrative example uses the discretization scheme given by Monaco and Normand-Cyrot. To demonstrate the existence of more than one pseudo-orbit, the same procedure used

for the first two examples was followed. To this end, consider the following discretized equation for the variable  $x$  of the Lorenz (Eq. (15)) by applying the Monaco and Normand-Cyrot scheme in Eq. (6) for  $\eta = 3$ :

$$\begin{aligned} x_{k+1} = & x_k - \frac{h^2}{2} ((y_k - x_k)\sigma^2 + (y_k - x_k(\rho - z_k))\sigma) \\ & + \frac{h^3}{6} (y_k - x_k(\rho - z_k))(\sigma^2 + \sigma) - \sigma h(x_k - y_k) \\ & - \frac{h^3}{6} \sigma(x_k - y_k)(\sigma^2 + (\rho - z_k)\sigma) + \frac{h^3}{6} \sigma x_k(\beta z_k - x_k y_k) \end{aligned} \tag{19}$$

Now consider two equivalent interval extension of Eq. (19):

$$\begin{aligned} x_{1,k+1} = & x_{1,k} - \frac{h^2}{2} (y_{1,k} - x_{1,k})\sigma^2 + (y_{1,k} - x_{1,k}(\rho - z_{1,k}))\sigma \\ & + \frac{h^3}{6} (y_{1,k} - x_{1,k}(\rho - z_{1,k}))(\sigma^2 + \sigma) - \sigma h(x_{1,k} - y_{1,k}) \\ & - \frac{h^3}{6} \sigma(x_{1,k} - y_{1,k})(\sigma^2 + (\rho - z_{1,k})\sigma) \\ & + \frac{h^3}{6} \sigma x_{1,k}(\beta z_{1,k} - x_{1,k} y_{1,k}) \end{aligned} \tag{20}$$

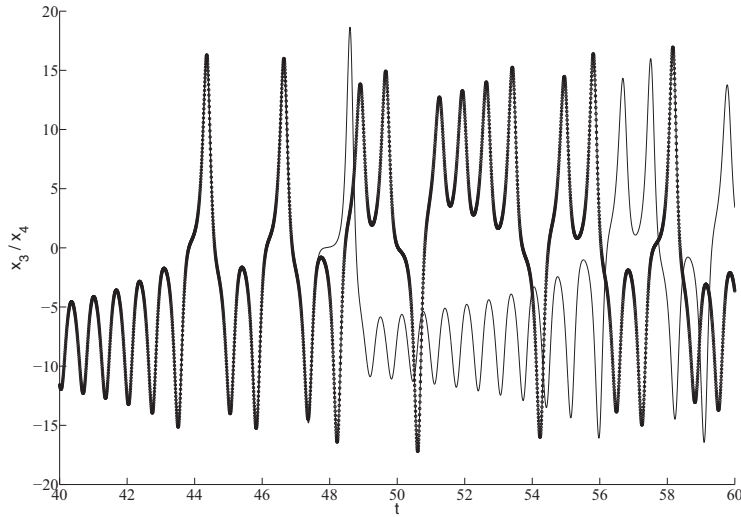


**Fig. 4.** Result of simulation for  $x_3$  (—) and  $x_4$  (---). The simulation is performed using the set of Eq. (16) for  $x_3$  and  $x_4$ . The difference is that for  $x_3$ , the original ode4 code was used and for  $x_4$  a slight difference on the code was implemented. The parameters  $\sigma = 10$ ,  $\rho = 28$ ,  $\beta = 8/3$ , initial conditions  $(x_0, y_0, z_0) = (0, 1, 1.05)$  and step-size  $h = 0.005$  are exactly the same.

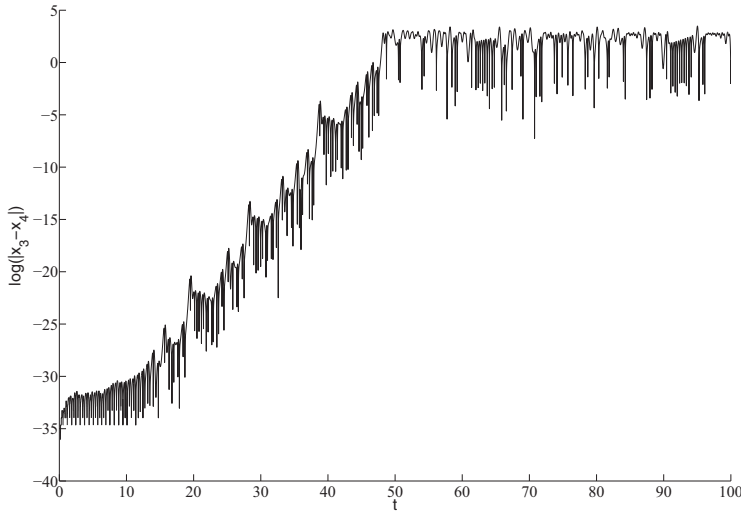


**Fig. 5.** Exponentially growing of the difference between the two pseudo-orbits  $x_3$  and  $x_4$ , as seen in Fig. 4.

and

$$\begin{aligned}
 x_{2,k+1} = & x_{2,k} - \frac{h^2}{2} (\underline{y_{2,k} - x_{2,k}}) \underline{\sigma\sigma} + (y_{2,k} - x_{2,k}(\rho - z_{2,k}))\sigma \\
 & + \frac{h^3}{6} (y_{2,k} - x_{2,k}(\rho - z_{2,k}))(\sigma^2 + \sigma) - \sigma h(x_{2,k} - y_{2,k}) \\
 & - \frac{h^3}{6} \sigma(x_{2,k} - y_{2,k})(\sigma^2 + (\rho - z_{2,k})\sigma) \\
 & + \frac{h^3}{6} \sigma x_{2,k}(\beta z_{2,k} - x_{2,k} y_{2,k})
 \end{aligned} \tag{21}$$

The difference between Eqs. (20) and (21) is that in the former one writes  $\sigma^2$  and in the latter  $\sigma\sigma$ , as indicated by an underline. As in the previous results, the two pseudo-orbits diverge from each other (Fig. 6) and after around  $t = 50$  LTU, the magnitude of the error is of the same magnitude of the state variable, as seen in Fig. 7.

The question that arises from the analysis of these examples is: with the same initial condition, same scheme of discretization and equivalent set of differential equations, which orbit is the true one? This is not an easy question to answer, since there is always no option but to use finite precision machine. Even the precision of the machine is increased as performed by Liao and Wang [24],

similar problems can occur. Although symbolic computation can be considered, the problem of iterating functions can be easily become intractable, although with advent of powerful computing systems the limit beyond the point where the trajectories diverge has been set further away (but it is still finite) [20,21,23].

One extreme consequence of such problems is that when the simulation reaches a value where level of error is high, and without any further analysis, the whole process should be carefully analysed (See Section 4.6). The basic explanation is that after this value there is no guarantee that a fixed point or cycle limit, or any other periodical orbital has been reached.<sup>1</sup> This is the very same issue already discussed in [39,40]. On the practical side this reveals the great importance of having access to the code used in a research work. Without the code, it may be impossible to reproduce the results.

<sup>1</sup> Despite being in a different context, some interesting and not intuitive bifurcation diagram of the photo conductor model is shown in [49] where the bifurcation parameter is the time duration of the simulation. The main result shown in that paper is that the time solution using a discretization scheme changes with time and can show a chaotic window even when it is known that the original systems does not exhibit it.

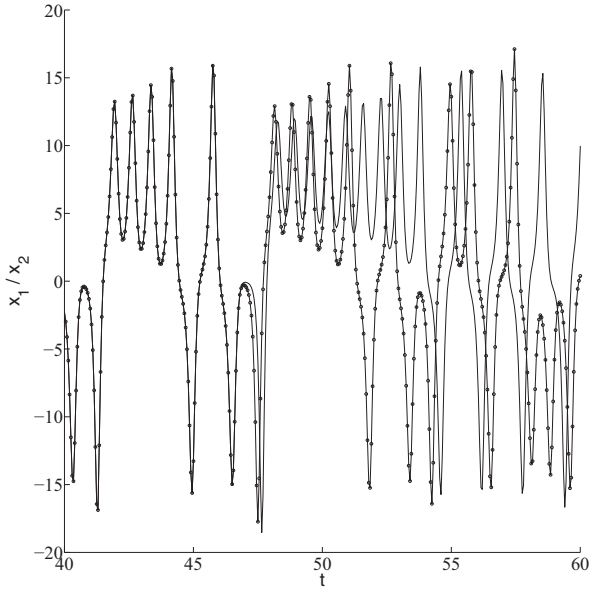


**Fig. 6.** Result of simulation for  $x_1$  (–) and  $x_2$  (–o–) according to Eqs. (20) and (21). The parameters are  $\sigma = 10$ ,  $\rho = 28$ ,  $\beta = 8/3$ , initial conditions  $(x_0, y_0, z_0) = (0.1, 0, 0)$  and step-size  $h = 0.01$  are the same for  $x_1$  and  $x_2$ .

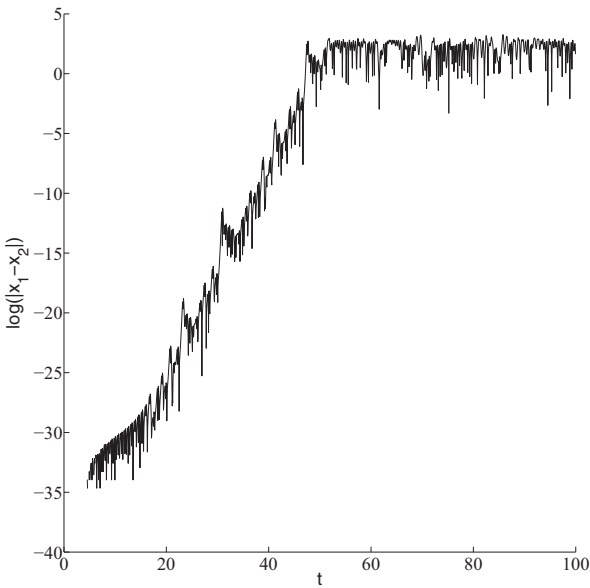


**Fig. 7.** Exponentially growing of the difference between the two pseudo-orbits  $x_1$  and  $x_2$  according to Eqs. (20) and (21).

**4.4. Equivalent interval extensions, data precision and positive Lyapunov exponent**

In this section the following interval extension of Eq. (15), different from the extensions on Eqs. 16 and 17, will be considered i) to illustrate the influence of the data precision chosen when simulating the Lorenz system and ii) to establish the connection of the pseudo-orbits to the positive Lyapunov exponent.

$$\begin{aligned}
 \frac{dx_4}{dt} &= \sigma(y_4 - x_4) \\
 \frac{dy_4}{dt} &= x_4(\rho - 1) + x_4 - x_4z_4 - y_4 \\
 \frac{dz_4}{dt} &= x_4y_4 - \beta z_4
 \end{aligned}
 \tag{22}$$

Typically the dynamical behaviour of nonlinear systems can be quantified by the so-called Lyapunov exponents spectrum, since the exponent values measure the divergence or convergence rates of trajectories in the directions of the flow [54]. In order to verify the existence of chaotic behaviour from time-series originated from the solution of a nonlinear system, the methods available in the literature estimate the positive Lyapunov exponent [16,17,44]. A rather simple modification of the algorithm proposed in [16,44] will be used here to estimate the positive Lyapunov exponent using interval extensions of the system under investigation [31].

In order to simulate Eq. 22 and the original system in Eq. 15, the RK4 method implemented in Fortran 90 was used. Two different compilers, Gnu-Fortran (gfortran) and ifort-Intel®, for both linux and OS operational systems were used and 32, 64 and 128 bit precisions were considered. Depending on the version of the compilers, gfortran and ifort® differ from each other on the 128 bit implementation (the latter shows a higher precision). It should be pointed out that the compilers can internally manipulate the code for optimization which can lead to a different or an equal interval extension.<sup>2</sup> Since the results for both compilers and operational systems are quite similar, only the results for the GNU compiler running on a linux machine are shown for the Lorenz example.

Fig. 8 shows the exponential growth of the difference between the trajectories for the Lorenz system in Eqs. 15 and 22, considering 128, 64 and 32 bit for the precision and step size  $h = 0.00001$ . The only step necessary to estimate the Lyapunov exponent is to fit a line equation to the region where the exponential growth is noticeable. The value of the exponent is the slope of the estimated equation. For higher precisions, that is, for 128 and 64 bits, the estimated exponent,  $\lambda \approx 0.94$ , is in good agreement with the value reported in [52, p. 62] as  $\lambda = 0.9056$ . For 32 bit precision, the exponential growth is also clear but the estimate of the Lyapunov exponent is no longer close to the value reported in the literature, although it is still positive. This seems to indicate that the 32 bit precision is not suitable for simulating the Lorenz equations.

Although it could be argued that the step size is too small, Fig. 9 shows that the results, when step size is  $h = 0.001$ , remain practically the same. Further simulations shows that is the case when the step size is reasonably increased. Note that the starting point where the trajectories start to diverge vary with the chosen precision.

To show that the equivalent interval extensions can be used to reliably estimate the positive Lyapunov exponent consider the Rossler hyperchaos system [45]:

$$\begin{aligned}
 \frac{dx_1}{dt} &= -y_1 + z_1 \\
 \frac{dy_1}{dt} &= x_1 + ay_1 + w_1 \\
 \frac{dz_1}{dt} &= b + x_1y_1 \\
 \frac{dw_1}{dt} &= cw_1 - dz_1
 \end{aligned}
 \tag{23}$$

where  $a = 0.25$ ,  $b = 3$ ,  $c = 0.05$ ,  $d = 0.5$  and the initial conditions are set to  $(x_1(0), y_1(0), z_1(0), w_1(0)) = (-10, 6, 0, 10)$ . To estimate the positive Lyapunov exponents the two equivalent interval extensions were simulated using a RK4 algorithm, the ifort® compiler installed on a mac system, 128 bit precision and step size  $h = 0.001$ .

<sup>2</sup> That is specially true for ifort®.

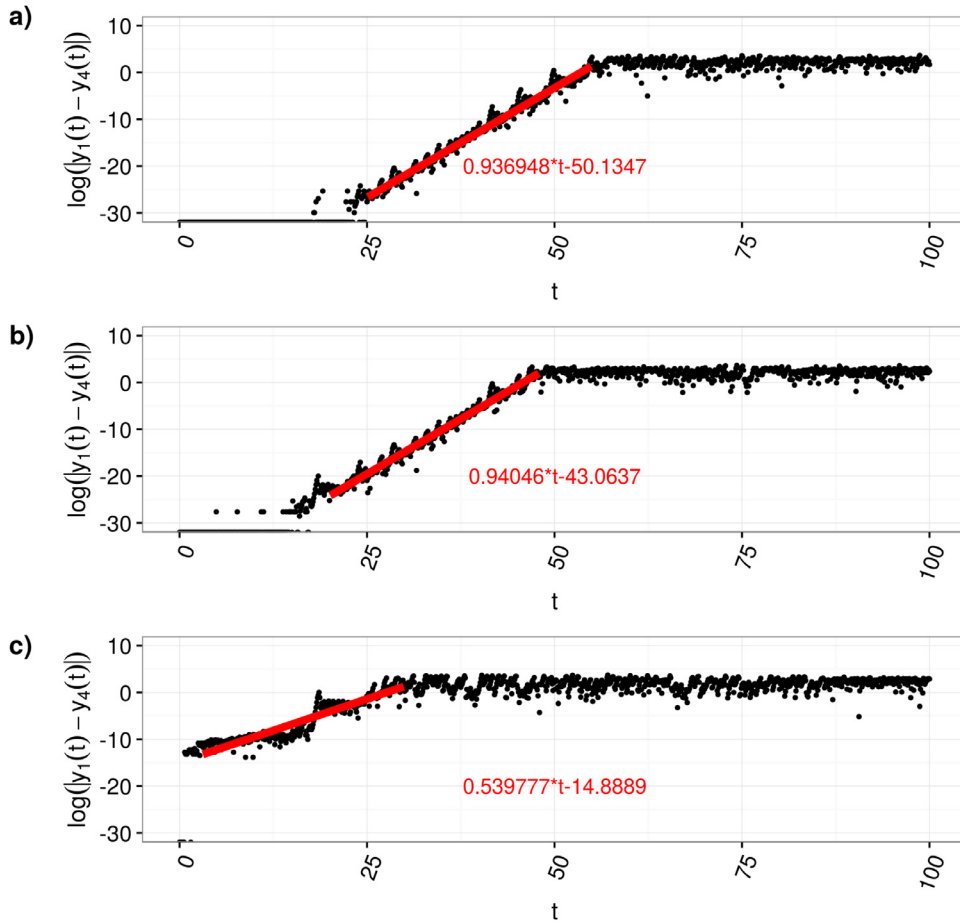


**Fig. 8.** Exponentially growing of the difference between the two pseudo-orbits  $y_1$  and  $y_4$  for a) 128 bits, b) 64 bits and c) 32 bits, and step size  $h = 0.00001$ . The slope of the equation for the linear regression of the region where the exponential growth is evident is in good agreement with the results in the literature for higher precisions. The parameters  $\sigma = 10$ ,  $\rho = 28$ ,  $\beta = 8/3$  and the initial conditions  $(x_0, y_0, z_0) = (0.1, 0, 0)$  are exactly the same.

$$\begin{aligned} \frac{dx_2}{dt} &= -y_2 + z_2 \\ \frac{dy_2}{dt} &= x_2 + ay_2 + w_2 \\ \frac{dz_2}{dt} &= b + x_2(z_2 + e) - ex_2 \\ \frac{dw_2}{dt} &= cw_2 - dz_2 \end{aligned} \quad (24)$$

and

$$\begin{aligned} \frac{dx_3}{dt} &= -y_3 + z_3 \\ \frac{dy_3}{dt} &= (x_3 - e) + e + ay_3 + w_3 \\ \frac{dz_3}{dt} &= b + x_3y_3 \\ \frac{dw_3}{dt} &= cw_3 - dz_3 \end{aligned} \quad (25)$$

where the dummy parameter  $e$  is set 1.

Fig. 10 shows the exponential growth due to the simulation of Eqs. 23–25 even when the step, the discretization algorithm, RK4, and the initial conditions are kept unchanged. The estimate of the positive Lyapunov exponent ( $\lambda \approx 0.11$ ) is very close to the value reported in [52, p. 153], that is,  $\lambda = 0.1120$ .

#### 4.5. The Mackey–Glass equation

In this subsection an example based on the Mackey–Glass equation is presented. This is an interesting system used in many papers as an example of a chaotic and infinite dimensional system, since it is a time-delay system [7,29]. The equation is given by

$$\dot{x}_1(t) = \frac{ax_1(t - \tau)}{1 - x_1(t - \tau)^c} - bx_1(t) \quad (26)$$

where  $a = 0.2$ ,  $b = 0.1$ ,  $c = 10$ ,  $\tau = 30$  with initial condition  $x(0) = 0.3$ . The simulation was carried out on Matlab environment using RK4 with integration step of 0.3 s. It was necessary 13,728 points to estimate the largest Lyapunov exponent as 0.0074, which is very close to the value reported in the literature (See [47]). To achieve that, the following interval extension was used

$$\dot{x}_2(t) = a \left( \frac{x_2(t - \tau)}{1 - x_2(t - \tau)^c} \right) - bx_2(t). \quad (27)$$

In this example, the critical time  $N_c$  is also calculated. From the generated time-series, the diameter of phase space and the positive Lyapunov exponent (using natural base) can be estimated as  $D = 1.381$  and  $\lambda = 0.0074$ , respectively. The precision is  $P = 16$  since the simulations were performed on a 64-bit platform. Finally, the critical time can be determined as

$$N_c = \frac{\log_{10}(1.381/2) + \log(10^{16})}{0.0074} = 4902. \quad (28)$$

The critical time clearly indicates the end of exponential growing of the lower bound error as can be seen in Fig. 11. This has



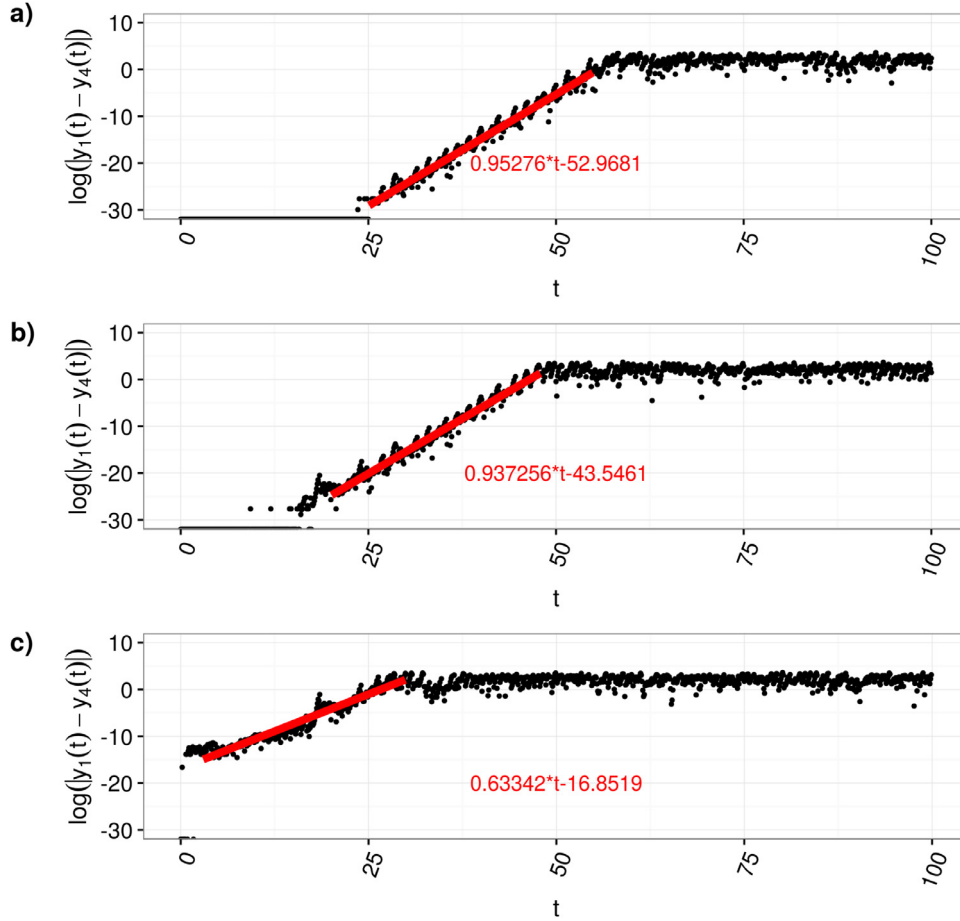


**Fig. 9.** Exponentially growing of the difference between the two pseudo-orbits  $y_1$  and  $y_4$  for a) 128 bits, b) 64 bits and c) 32 bits, and step size  $h = 0.001$ . The slope of the equation for the linear regression of the region where the exponential growth is evident is in good agreement with the results in the literature for higher precisions. The parameters  $\sigma = 10$ ,  $\rho = 28$ ,  $\beta = 8/3$  and the initial conditions  $(x_0, y_0, z_0) = (0.1, 0, 0)$  are exactly the same.

two important consequences. First, the simulation can be trusted, at most, up to  $t = N_c$  from the numerical point of view. Second, the critical time determines the reliable chunk of data that can be used for the estimation of the positive Lyapunov exponent.

Although it has been shown that the equivalent interval extensions can be used to estimate the positive Lyapunov exponent, care should be taken to generalize such results. Section 4.6 will show that two interval extensions of the Sprott A system can lead to completely different outcomes which emphasizes the main point of this work.

#### 4.6. The Sprott A example

In order to show that the solutions of the equivalent interval extensions may be different altogether and not a solution due to a parameter displacement [19], consider the conservative system proposed independently by William Graham Hoover and Julien Clinton Sprott [12,15,38,51,52]:

$$\begin{aligned} \frac{dx}{dt} &= y \\ \frac{dy}{dt} &= yz - x \\ \frac{dz}{dt} &= 1 - y^2. \end{aligned} \tag{29}$$

Despite the simplicity, the so-called Sprott A system has interesting features such as no fixed points and volume preservation. Applying the Normand-Cyrot discretization scheme of third order

to the system in Eq. 29 and considering two equivalent interval extensions yields to the following discretized models:

$$\begin{aligned} x_{1,k+1} &= (6 \times x(1, k) - 3 \times h^2 \times x(1, k) \\ &\quad + 6 \times h \times y(1, k) - h^3 \times y(1, k)^3 \\ &\quad - h^3 \times x(1, k) \times z(1, k) + 3 \times h^2 \times y(1, k) \times z(1, k) \\ &\quad + h^3 \times y(1, k) \times z(1, k)^2)/6. \\ y_{1,k+1} &= (-6 \times h \times x(1, k) - h^3 \times x(1, k) + 6 \times y(1, k) \\ &\quad + 4 \times h^3 \times x(1, k) \times y(1, k)^2 \\ &\quad - 3 \times h^2 \times y(1, k)^3 - 3 \times h^2 \times x(1, k) \times z(1, k) \\ &\quad + 6 \times h \times y(1, k) \times z(1, k) \\ &\quad + h^3 \times y(1, k) \times z(1, k) - 5 \times h^3 \times y(1, k)^3 \\ &\quad \times z(1, k) - h^3 \times x(1, k) \times z(1, k)^2 \\ &\quad + 3 \times h^2 \times y(1, k) \times z(1, k)^2 + h^3 \times y(1, k) \times z(1, k)^3)/6. \\ z_{1,k+1} &= (3 \times h - h^3 \times x(1, k)^2 + 3 \times h^2 \times x(1, k) \times y(1, k) \\ &\quad - 3 \times ts \times y(1, k)^2 + h^3 \times y(1, k)^4 + 3 \times z(1, k) \\ &\quad + 3 \times h^3 \times x(1, k) \times y(1, k) \times z(1, k) \\ &\quad - 3 \times h^2 \times y(1, k)^2 \times z(1, k) \\ &\quad - 2 \times h^3 \times y(1, k)^2 \times z(1, k)^2)/3. \end{aligned} \tag{30}$$

and

$$\begin{aligned} x_{2,k+1} &= (-(x(2, k) \times (-6 + h^2 \times (3 + h \times z(2, k)))) \\ &\quad + h \times y(2, k) \times (6 + 3 \times h \times z(2, k) \\ &\quad + h^2 \times (-y(2, k)^2 + z(2, k)^2)))/6. \end{aligned}$$

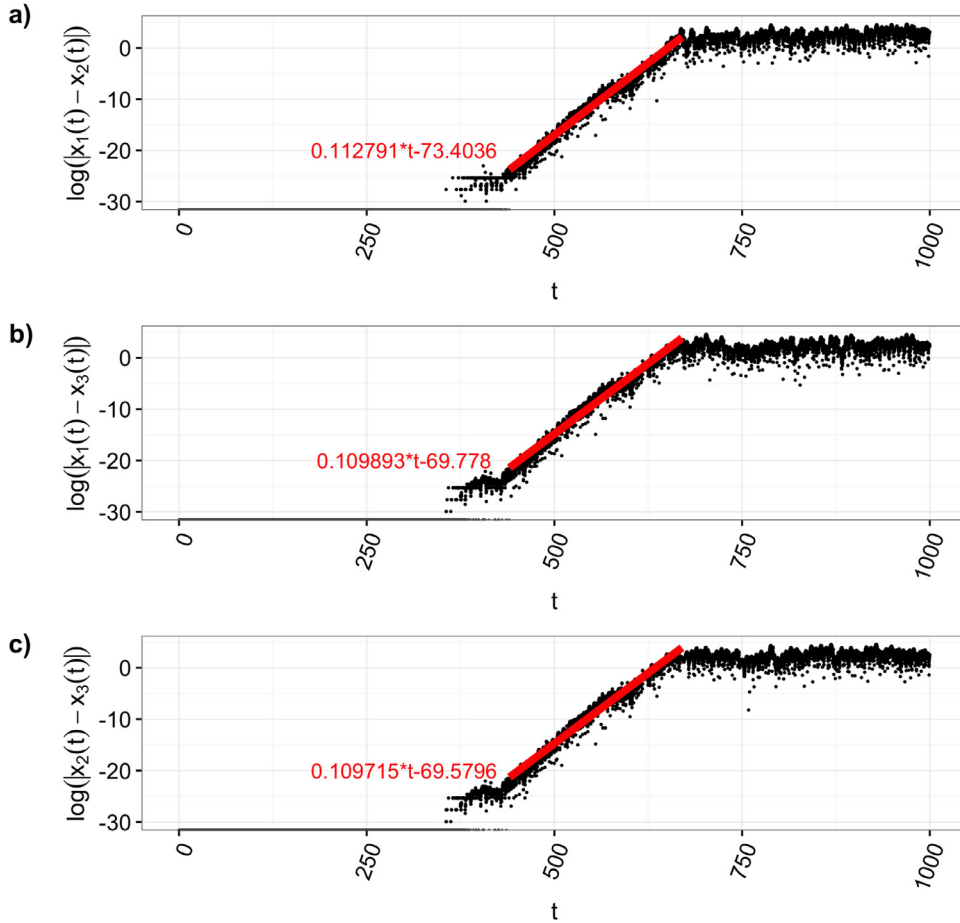


**Fig. 10.** Estimation of the positive Lyapunov exponent using equivalent interval extensions for the Rossler hyperchaos system in Eq. 23. The equations were simulated using a RK4 algorithm coded in Fortran 90 and compiled using the *ifort*<sup>®</sup> compiler. Step-size  $h = 0.001$  and 128 bit precision. X-coordinate, error between: a) Eqs. 23 and 24, b) Eqs. 23 and 25 and c) Eqs. 24 and 25. The parameters are  $a = 0.25$ ,  $b = 3$ ,  $c = 0.05$ ,  $d = 0.5$  and the initial conditions are set to  $(x_1(0), y_1(0), z_1(0), w_1(0)) = (-10, 6, 0, 10)$ .

$$\begin{aligned}
 y_{2,k+1} &= (6 \times y(2, k) + h \times (x(2, k) \times (-6 - h \times (3 \times z(2, k) \\
 &\quad + h \times (1 - 4 \times y(2, k)^2 + z(2, k)^2))) + y(2, k) \\
 &\quad \times (6 \times z(2, k) + h \times (-y(2, k)^2 \times (3 + 5 \times h \times z(2, k))) \\
 &\quad + z(2, k) \times (h + 3 \times z(2, k) + h \times z(2, k)^2))))/6. \\
 z_{2,k+1} &= h - h \times y(2, k)^2 + z(2, k) + h^2 \times y(2, k) \\
 &\quad \times (x(2, k) - y(2, k) \times z(2, k)) + \\
 &\quad (h^3 \times (y(2, k)^4 - (x(2, k) - 2 \times y(2, k) \\
 &\quad \times z(2, k)) \times (x(2, k) - y(2, k) \times z(2, k))))/3. \quad (31)
 \end{aligned}$$

The choice of the Normand-Cyrot discretization scheme is based on a recent recommendation in [8] where the author states that the Taylor models could be an interesting alternative for circumvent the long term integration of nonlinear dynamical systems although they are not available in most widespread software packages. The Normand-Cyrot is simply the Taylor method in a short formulation. Furthermore Letellier et al. [19] showed that this method has outperformed other available methods in the case of numerically finding the solution for conservative systems.

Mathematically Eq. (30) and (31) are the same. For small values of the step size  $h$ , both equations can reproduce the original Poincarè section ( $z = 0$ ). However when the step size is increased and reaches  $h = 3.74095 \times 10^{-01}$  (double precision used in the Fortran code), the Poincarè Sections are no longer representative of the original section but more importantly they differ from each other. The first Poincarè shown in Fig. 12 a) was built using

2,000,000 crossing points<sup>3</sup> and there is no sign that the trajectory will eject to infinity. In the second Poincarè section, the trajectory ejects to infinity after only 768 crossings.<sup>4</sup> This clearly shows that one of the equivalent interval extension resulted in stability of the solution and the other one in instability and as a result the two solutions no longer are topologically equivalent. Therefore the proposed method can also aid the user of discretization schemes to choose the range of step sizes when the main consideration is to faithfully reproduce the original dynamics.

## 5. Conclusions

This paper has demonstrated the existence of multiple pseudo-orbits for nonlinear dynamics systems when discretization schemes are used even when the step-size is not varied and the initial conditions are kept unchanged. As examples the Lorenz equations, the Rossler hyperchaos system, the Mackey–Glass equation and the Sprott A system were investigated and it was shown that simple changes on the differential equations or in the equations of numerical method produce different outcomes, even if parameters and initial conditions are kept the same. The bit resolution, the step size value and the compiler used were also investigated. As a consequence a lower bound error and a critical time based on the very definition of pseudo-orbits and on the assump-

<sup>3</sup> 7,429,765 iteration of Eq. 30.

<sup>4</sup> 2,147,483,647 iterations of Eq. 31.

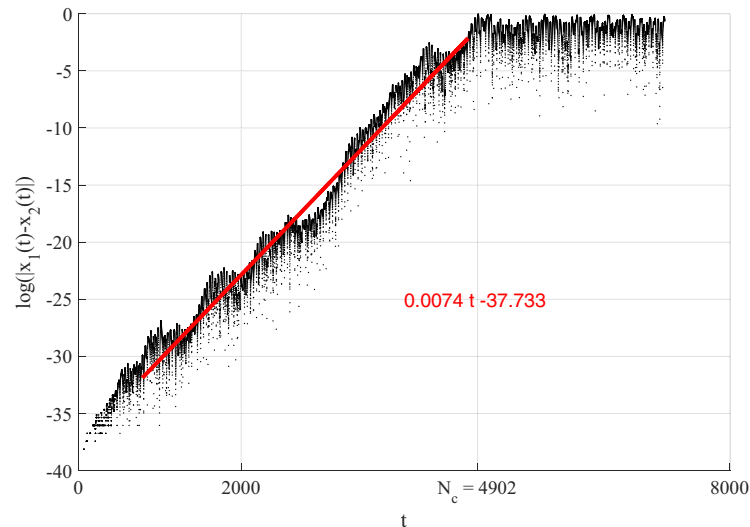


**Fig. 11.** Estimation of the positive Lyapunov exponent using equivalent interval extensions for the Mackey–Glass system in Eq. (26). The equations were simulated using a RK4 algorithm coded in Matlab R2016 with step-size  $h = 0.3$  and 64 bit precision. X-coordinate, error between: a) Eqs. (26) and (27). The parameters are  $a = 0.2$ ,  $b = 0.1$ ,  $c = 10$ ,  $\tau = 30$  with initial condition  $x(0) = 0.3$ . The critical time  $N_c$ , calculated by Eq. 28 is indicated on the x-axis.

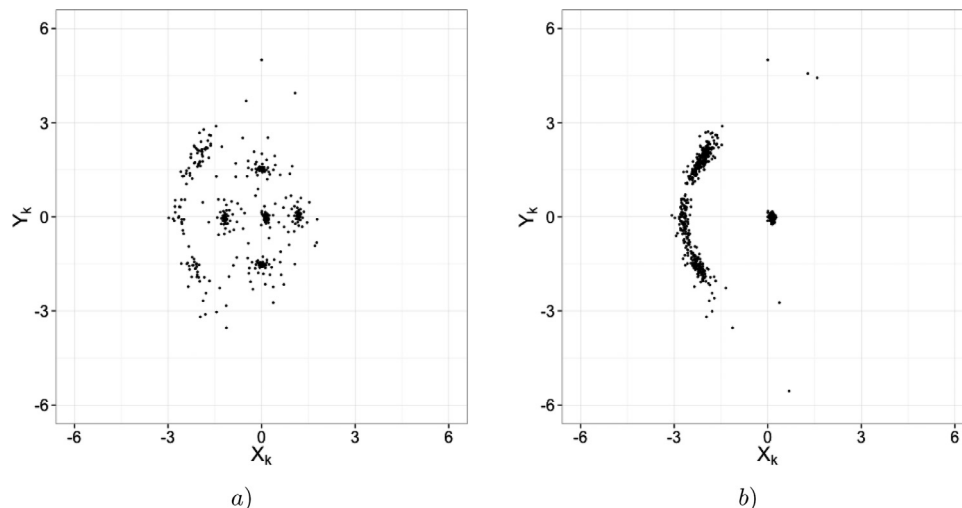


**Fig. 12.** Poincaré sections considering the crossing at  $z = 0$  for a) Eq. 30 and b) Eq. 31. The Normand-Cyrot discretization scheme (Fortran, *gfortran*, double precision) was used with step-size  $h = 3.74095 \times 10^{-01}$  and initial conditions  $(x_0, y_0, z_0) = (0, 5, 0)$ .

tion that after a long period of simulation the error of pseudo-orbits grows was proposed to help the user of the discretization schemes.

Although a solution for this problem based on earlier papers dealing with the linear case was not provided, some different facets of the nonlinear case have been characterized and analysed. On one side if the user of discretization schemes knows that his/her simulation reaches an error value as shown in the illustrative examples, his/her objective and even the reliability of numerical result could be questioned. On the other side it has been demonstrated that the maximum (positive) Lyapunov exponent can be easily estimated using two pseudo-orbits, when the parameters for the simulation such as step-size and resolution (precision) are judiciously chosen. The same goes for the critical time, which indicates the range of reliable data used for simulation purposes or for the estimation of the Lyapunov Exponent, when two pseudo-orbits reach the maximum distance between them.

It has also been shown that the solutions originated from two equivalent interval extensions for the same system, with the same initial conditions and step size, can be so different that one trajectory ejects to infinity and the other does not. This outcome

could be used as an aid to the user of discretization schemes when choosing the step size.

Finally it is worth emphasizing the importance to have access to the code used for simulation. As there is no equivalence between mathematical equations and interval extensions, it may be impossible to reproduce and check results in the literature.

Future research is intended to be made in two directions: generalization of the results of the lower bound error for the case of more than two pseudo-orbits and deeper knowledge on how the error propagates when simulating continuous nonlinear dynamic systems when a lower bit resolution is considered.

### Acknowledgements

This work has been supported by CNPq/INERGE, Fapemig and Capes.

### References

- [1] Banks J, Brooks J, Cairns G, Davis G, Stacey P. On Devaney's definition of chaos. *Am Math Monthly* 1992;99(4):332.

- [2] Bastos SB, Mendes EMAM. Dynamic valid models for the conservative Hénon-Heiles system. *J Phys Conf Ser* 2011;285(1):012027.
- [3] Billings SA. *Nonlinear system identification: NARMAX methods in the time, frequency, and spatio-temporal domains*. West Sussex: John Wiley & Sons; 2013.
- [4] Bomar BW. Low-roundoff-noise limit-cycle-free implementation of recursive transfer functions on a fixed-point digital signal processor. *IEEE Trans Ind Electron* 1994;41(1):70–8. doi:10.1109/41.281610.
- [5] Corless RM. What good are numerical simulations of chaotic dynamical systems? *Comput Math Appl* 1994;28(10):107–21. [http://dx.doi.org/10.1016/0898-1221\(94\)00188-X](http://dx.doi.org/10.1016/0898-1221(94)00188-X).
- [6] Faranda D, Mestre M, Turchetti G. Analysis of round off errors with reversibility test as a dynamical indicator. *Int J Bifurcation Chaos* 2012;22(9):1250215.
- [7] Farmer JD. Chaotic attractors of an infinite-dimensional dynamical system. *Physica D* 1982;4(3):366–93.
- [8] Galias Z. The dangers of rounding errors for simulations and analysis of nonlinear circuits and systems? and how to avoid them. *IEEE Circuits Syst Mag* 2013;13(3):35–52.
- [9] Gilmore R, Lefranc M. *The topology of chaos: alice in stretch and squeeze land*. John Wiley & Sons; 2012.
- [10] Goldberg D. What every computer scientist should know about floating-point arithmetic. *Comput Surv* 1991;23(1):5–48.
- [11] Hammel S, Yorke J, Grebogi C. Do numerical orbits of chaotic dynamical processes represent true orbits? *J Complex* 1987;3(2):136–45.
- [12] Hoover WG, Hoover CG, Sprott JC. Nonequilibrium systems: hard disks and harmonic oscillators near and far from equilibrium. *Mol Simul* 2016;42:1300–16. doi:10.1080/08927022.2015.1086999.
- [13] Jackson L. Limit cycles in state-space structures for digital filters. *IEEE Trans Circuits Syst* 1979;26(1):67–8. doi:10.1109/tcs.1979.1084547.
- [14] Jackson LB. On the interaction of roundoff noise and dynamic range in digital filters\*. *Bell Syst Tech J* 1970;49(2):159–84. doi:10.1002/j.1538-7305.1970.tb01763.x.
- [15] Jafari S, Sprott JC, Hashemi Golpayegani SMR. Elementary quadratic chaotic flows with no equilibria. *Phys Lett A* 2013;377(9):699–702. doi:10.1016/j.physleta.2013.01.009.
- [16] Kantz H. A robust method to estimate the maximal lyapunov exponent of a time series. *Phys Lett A* 1994;185(1):77–87. doi:10.1016/0375-9601(94)90991-1.
- [17] Kim BJ, Choe GH. High precision numerical estimation of the largest lyapunov exponent. *Commun Nonlinear Sci Numer Simul* 2010;15(5):1378–84. doi:10.1016/j.cnsns.2009.05.064.
- [18] Lao S. On the reliability of computed chaotic solutions of non-linear differential equations. *Tellus A* 2009;61:550–64.
- [19] Letellier C, Mendes EMAM, Mickens RE. Nonstandard discretization schemes applied to the conservative Hénon-Heiles system. *Int J Bifurcation Chaos* 2007;17(3):891–902. doi:10.1142/S0218127407017616.
- [20] Liao S. Chaos: a bridge from microscopic uncertainty to macroscopic randomness. *Commun Nonlinear Sci Numer Simul* 2012;17(6):2564–9. doi:10.1016/j.cnsns.2011.10.033.
- [21] Liao S. On the numerical simulation of propagation of micro-level inherent uncertainty for chaotic dynamic systems. *Chaos Solit Fract* 2013;47:1–12. doi:10.1016/j.chaos.2012.11.009.
- [22] Liao S. Can we obtain a reliable convergent chaotic solution in any given finite interval of time? *Int J Bifurcation Chaos* 2014a;24(09):1450119. doi:10.1142/s0218127414501193.
- [23] Liao S. Physical limit of prediction for chaotic motion of three-body problem. *Commun Nonlinear Sci Numer Simul* 2014b;19(3):601–16. doi:10.1016/j.cnsns.2013.07.008.
- [24] Liao S, Wang P. On the mathematically reliable long-term simulation of chaotic solutions of Lorenz equation in the interval [0,10000]. *Sci China* 2014;57(2):330–5.
- [25] Lorenz EN. Deterministic nonperiodic flow. *J Atmos Sci* 1963;20:283–93.
- [26] Lorenz EN. Computational chaos - a prelude to computational instability. *Physica D* 1989;35:299–317.
- [27] Lorenz EN. Computational periodicity as observed in a simple system. *Tellus* 2006;58A:549–57.
- [28] Lozi R. Can we trust in numerical computations of chaotic solutions of dynamical systems?. In: Christophe L, editor. *Topology and dynamics of chaos: in celebration of Robert Gilmore's 70th birthday*, vol. 1. World Scientific Publishing Co. Pte. Ltd.; 2013. p. 63–98.
- [29] Mackey M, Glass L. Oscillation and chaos in physiological control systems. *Science* 1977;197(4300):287–9.
- [30] Mendes EMAM, Billings SA. A note on discretization of nonlinear differential equations. *Chaos* 2002;12(1):66–71. doi:10.1063/1.1445783.
- [31] Mendes EMAM, Nepomuceno EG. A very simple method to calculate the (positive) Largest Lyapunov Exponent using interval extensions. *Int J Bifurcation Chaos* 2016:Accepted.
- [32] Mills W, Mullis C, Roberts R. Digital filter realizations without overflow oscillations. *IEEE Trans Acoust* 1978;26(4):334–8. doi:10.1109/tassp.1978.1163114.
- [33] Monaco S, Normand-Cyrot D. A combinatorial approach of the nonlinear sampling problem. In: 9th international conference on analysis and optimization of systems, Antibes, France, Jun 12–15, 1990. In: *Lecture notes in control and information sciences*, 144; 1990. p. 788–97.
- [34] Moore B. Principal component analysis in linear systems: controllability, observability, and model reduction. *IEEE Trans Automat Control* 1981;26(1):17–32. doi:10.1109/tac.1981.1102568.
- [35] Moore RE, Moore RE. *Methods and applications of interval analysis*, vol. 2. Philadelphia: SIAM; 1979.
- [36] Mullis C, Roberts R. Finite-memory problems and algorithms. *IEEE Trans Inf Theory* 1974;20(4):440–55. doi:10.1109/tit.1974.1055258.
- [37] Mullis C, Roberts R. Roundoff noise in digital filters: frequency transformations and invariants. *IEEE Trans Acoust* 1976;24(6):538–50. doi:10.1109/tassp.1976.1162869.
- [38] Munmuangsaen B, Sprott JC, Thio WJ-C, Buscarino A, Fortuna L. A simple chaotic flow with a continuously adjustable attractor dimension. *Int J Bifurcation Chaos* 2015;25(12):1530036. doi:10.1142/s0218127415300360.
- [39] Nepomuceno EG. Convergence of recursive functions on computers. *J Eng* 2014;1–3. doi:10.1049/joe.2014.0228.
- [40] Nepomuceno EG, Martins SAM. A lower bound error for free-run simulation of the polynomial NARMAX. *Syst Sci Control Eng* 2016;4(1):50–8. doi:10.1080/21642583.2016.1163296.
- [41] Ott E. *Chaos in dynamical systems*. Cambridge: Cambridge University Press; 2002.
- [42] Peck SL. Simulation as experiment: a philosophical reassessment for biological modeling. *Trends Ecol Evol* 2004;19(10):530–4.
- [43] Quarteroni A, Saleri F, Gervasio P. *Scientific computing with Matlab and Octave*, volume 2 de texts in computational science and engineering. Springer-Verlag, Berlin.; 2006.
- [44] Rosenstein MT, Collins JJ, De Luca CJ. A practical method for calculating largest Lyapunov exponents from small data sets. *Physica D* 1993;65(1–2):117–34. doi:10.1016/0167-2789(93)90009-p.
- [45] Rossler OE. An equation for hyperchaos. *Phys Lett A* 1979;71(2–3):155–7. doi:10.1016/0375-9601(79)90150-6.
- [46] Sandberg IW. Floating-point-roundoff accumulation in digital-filter realizations. *Bell Syst Tech J* 1967;46(8):1775–91. doi:10.1002/j.1538-7305.1967.tb03171.x.
- [47] Sano M, Sawada Y. Measurement of the Lyapunov spectrum from a chaotic time series. *Phys Rev Lett* 1985;55(10):1082–5.
- [48] Sauer T, Grebogi C, Yorke J. How long do numerical chaotic solutions remain valid? *Phys Rev Lett* 1997;79(1):59–62.
- [49] Serfaty de Markus A. Numerical crisis found in the fixed step integration of a photoconductor model. *Phys Rev E* 1997;56(1):88–93.
- [50] Sheng H. Roundoff noise in state-space digital filtering: a general analysis. *IEEE Trans Acoust* 1976;24(3):256–62. doi:10.1109/tassp.1976.1162802.
- [51] Sprott JC. Some simple chaotic flows. *Phys Rev E* 1994;50(2):R647–50. doi:10.1103/PhysRevE.50.R647.
- [52] Sprott JC. *Elegant chaos: algebraically simple chaotic flows*. Singapore: World Scientific; 2010. ISBN 978-283-881-3
- [53] Teixeira J, Reynolds CA, Judd K. Time step sensitivity of nonlinear atmospheric models: numerical convergence, truncation error growth, and ensemble design. *J Atmos Sci* 2007;64(1):175–89.
- [54] Wolf A, Swift JB, Swinney HL, Vastano JA. Determining lyapunov exponents from a time series. *Physica D* 1985;16(3):285–317. doi:10.1016/0167-2789(85)90011-9.